Proceedings of the 7th GACM Colloquium on Computational Mechanics
for Young Scientists from Academia and Industry
October 11-13, 2017 in Stuttgart, Germany

Shape optimization with application to inverse form finding and the use of mesh adaptivity

Michael Caspari[1]*, Philipp Landkammer[1] and Paul Steinmann[1]

Micro Abstract
The aim of our novel inverse form finding approach is to determine the optimized workpiece geometry to its given target geometry after a forming process. During the optimization procedure, deviations between the computed and the target spatial configuration have to be minimized, whereby material nodal positions serve as design variables. The shape optimization is applied to a notch stamping process. As a special feature, mesh adaptivity is applied within the iterative forming simulation.

[1]Chair of Applied Mechanics, Friedrich-Alexander Universität Erlangen-Nürnberg, Erlangen, Germany
***Corresponding author**: michael.caspari@fau.de

Introduction

Typically, metal forming processes are classified as i) sheet forming with plane stress and ii) bulk metal forming with three dimensional stress conditions. Sheet-Bulk Metal Forming (SBMF), a novel class of forming processes, combines sheet metal forming operations with three dimensional plastic flow. Hence, SBMF intends to form local shape elements normal to the sheet plane [7]. As usual in various fields of product development, optimization is also applied to SBMF processes in order to reduce experimental costs. In this contribution, numerical shape optimization aiming at inverse form finding is considered. Here, in contrast to the forming simulation, shape optimization is an inverse problem [3].

The inverse form finding strategy [6] seeks to determine the optimal workpiece geometry based on the forming simulation and the prescribed spatial target geometry. Nodal positions serve as design variables and the deviations between the nodal positions of the computed spatial configuration and the prescribed spatial target configuration enter into the objective function δ of the optimization, which has to be minimized during the optimization. Since it dos not require intervention to the FE code, the algorithm is non-invasive. Hence, various FE simulation tools considering different material behavior may be employed, whereby data transfer is ensured by subroutines.

Performing forming simulation often requires a trade-off between accuracy and computational cost. In particular high accuracy has to be achieved despite of friction, contact and large deformations which often lead to severe mesh distortions. Since a equal fine mesh throughout the entire model cause high computational cost adaptive strategies are used to refine the mesh locally according to the simulation progress and based on error estimators. Thus a sufficient accurate and smooth mesh is ensured. In the present contribution, an h-adaptivity offered by MSC Marc is used to refine the mesh locally in regions of severe distortions. H-adaptivity allows for more complex geometries and high local plastic strains.

In the following, a truncated version of the inverse form finding algorithm is introduced in Sec. 1. In Sec. 2, an example demonstrating the application of the algorithm for a notch stamping process is discussed. Finally, essential findings are summarized in Sec. 3

1 Inverse Optimization Approach

The shape optimization procedure is based on nonlinear continuum mechanics. The physical body is placed into the Euclidean space $\mathbb{E}^3$ and its material configuration is denoted by $\mathcal{B}_0$. In contrast, its spatial configuration for time $t > 0$ is labeled as $\mathcal{B}_t$. Position vectors $\boldsymbol{X}$ in $\mathcal{B}_0$ are mapped to position vectors $\boldsymbol{x}$ in $\mathcal{B}_t$ by means of the deformation map $\boldsymbol{\varphi}$ as

$$\boldsymbol{x} = \boldsymbol{\varphi}(\boldsymbol{X}, t) \quad : \mathcal{B}_0 \to \mathcal{B}_t \,. \tag{1}$$

A linear map from the material tangent space $T\mathcal{B}_0$ to the spatial tangent space $T\mathcal{B}_t$ is governed by the gradient $\boldsymbol{F}$ of the deformation map with respect to material coordinates:

$$\boldsymbol{F} = \frac{\partial \boldsymbol{\varphi}(\boldsymbol{X})}{\partial \boldsymbol{X}} \quad : T\mathcal{B}_0 \to T\mathcal{B}_t \tag{2}$$

For our node-based algorithm all quantitites has to be discretized in the same way as for FE method. For a detailed description of FEM we may refer among others to [1]. Positions of design nodes are denoted by $\boldsymbol{x}^D$, $D = 1, \ldots, n_{\text{dsgn}}$ and subsumed in column vectors $\mathbf{x}^{\text{D}} = [\boldsymbol{x}^{1\top}, \cdots, \boldsymbol{x}^{\text{dsgn}\top}]^\top$.

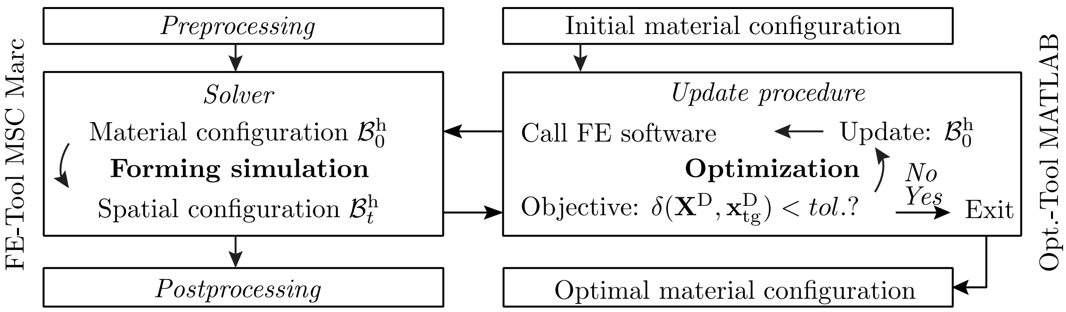

Figure 1. The iterative strategy for inverse form finding, separated into forming simulation (direct problem) and shape optimization (inverse problem) [5].

The optimization procedure is depicted in Fig 1. To realize a non-invasive approach the optimization is separated from the forming simulation. The algorithm for the update procedure is introduced in [6]. There, the objective function δ summarizes the local squared error of the nodal differences between the current spatial and prescribed spatial target configuration:

$$\delta(\mathbf{X}^{\text{D}}, \mathbf{x}_{\text{tg}}^{\text{D}}) = \sum_{D=1}^{n_{\text{dsgn}}} \delta^D \left(\boldsymbol{x}_{\text{tg}}^D, \boldsymbol{\varphi}(\boldsymbol{X}^D) \right) \tag{3}$$

$$\delta^D = \frac{1}{2} \boldsymbol{d}^{D\mathsf{T}} \cdot \boldsymbol{d}^D \quad \text{with} \quad \boldsymbol{d}^D = \boldsymbol{x}_{\text{tg}}^D - \boldsymbol{\varphi}(\boldsymbol{X}^D) \tag{4}$$

The update step is motivated by a minimization of the objective function to determine the optimal configuration $\mathbf{X}_{\text{opt}}^{\text{D}}$. A linear approximation by Taylor series terminated after the first term derives an iterative Newton step as

$$\boldsymbol{X}^D \leftarrow \boldsymbol{X}^D - \alpha \, \frac{\partial^2 \delta^D \left(\boldsymbol{X}^D, \boldsymbol{x}_{\text{tg}}^{\text{h}} \right)}{\partial \boldsymbol{X}^D \partial \boldsymbol{X}^D}^{-1} \cdot \frac{\partial \delta^D \left(\boldsymbol{X}^D, \boldsymbol{x}_{\text{tg}}^{\text{h}} \right)}{\partial \boldsymbol{X}^D} \,. \tag{5}$$

Finally, further approximations lead to an update step for each design node as

$$\boldsymbol{X}_{k+1}^D = \boldsymbol{X}_k^D - \alpha \, \tilde{\boldsymbol{F}}^{D^{-1}} \cdot \boldsymbol{d}^D \,. \tag{6}$$

The linesearch parameter α introduced in Eq. (5) ensures a suited update without severe mesh distortions and is controlled by Armijo-Backtracking [6]. A Least-Squares smoothing technique recommended by Hinton and Campbell [4] is applied to map quantities from the Gauss points of adjacent elements to the discretization node. The smoothed inverse deformation gradient $\tilde{\boldsymbol{F}}^{D^{-1}}$ is used to map the nodal difference vector of the considered node from the spatial to the material configuration in order to obtain an updated material configuration.

2 Example

The example is motivated by a notch stamping process employed in an investigation of the plastic flow in an incremental process of SBMF for gears [8] and has been recently discussed in [2]. The material configuration is depicted in Fig. 2(**a**). The bottom is fixed in e_2-direction and the boundary condition on the right side represents a symmetry condition in e_1-direction. The quadratic 2D-solid body is discretized by 64 quadrilateral elements (plane stress). The material model considers nonlinear isotropic hardening and its material parameters correspond to the dual phase steel DP600 as investigated by [10]. The contact body of the notch is reduced onto a horizontal and a 45° line. The notch penetrates at a constant velocity into the specimen up to 25 mm depth. Between the solid body and the notch a friction coefficient of 0.07 is used as in [9].

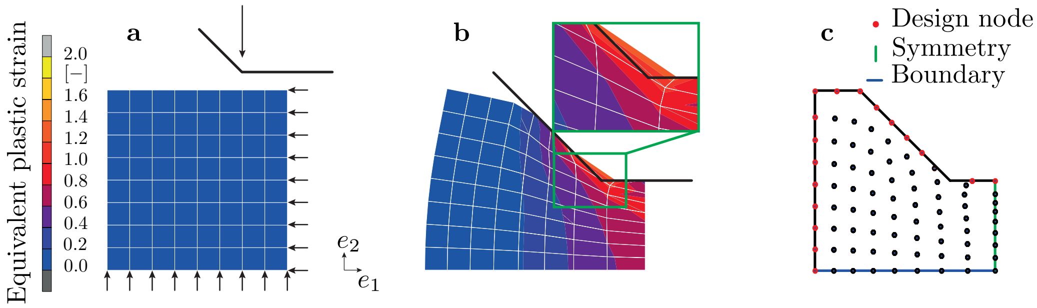

Figure 2. The original discretized material configurations (**a**) and the corresponding computed spatial configuration (**b**) in comparison to the target spatial configuration (**c**)

Fig. 2(**b**) shows the computed spatial configuration after the first simulation run. The target spatial configuration, depicted in Fig. 2(**c**), is approximated by the same number of nodes and elements but an exact imprint of the notch into the quadratic box is applied. The distinction between design-, symmetry- and boundary nodes is proposed by [5], for the inverse form finding approach. It enables to restrict the inverse update procedure to nodes representing the shape of the model. The optimization aims to reduce the deviations between the design nodes of the computed spatial (**b**) and target spatial configuration (**c**) by updating iteratively the material configuration (**a**).

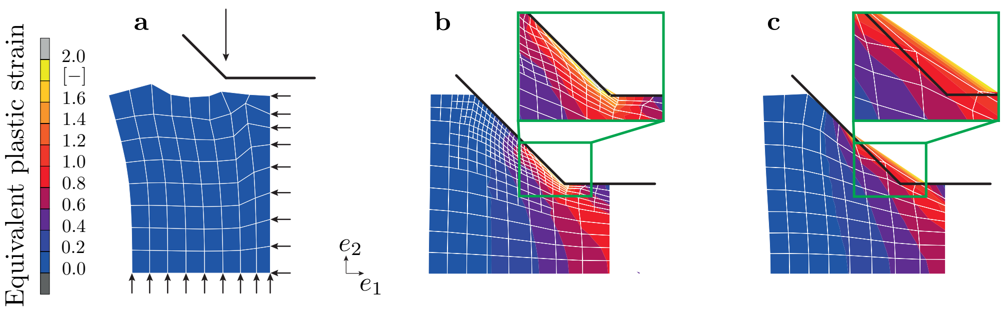

Figure 3. Updated material configuration (**a**), computed spatial configuration by use of h-adaptivity (**b**) and without refinement (**c**)

Fig. 3(**a**) depicts the optimized material configuration after four iterations. The shape is adapted to fit the spatial target configuration. The finally obtained spatial configuration is given in Fig. 3(**b**), whereby h-adaption is applied and consequently the severe distortions of the elements close to the intended notch are reduced, cf. the detailed view in Fig. 3(**b**) and Fig. 2(**b**), 3(**c**). The optimization without adaption leads to similar results of the final workpiece geometry, however, the corresponding spatial configuration in Fig. 3(**c**) shows severe element distortions. In this case plastic strains are not meaningful.

3 Conclusions

The inverse form finding algorithm determines the optimal workpiece geometry to a given forming simulation with respect to a desired spatial target configuration. With the help of the previous enhancements together with mesh adaptive strategies, the optimization procedure is applicable to material models including nonlinear material behavior and contact with sharp edges, whereby severe mesh distortions are avoided. The obtained spatial configuration fit into the target spatial configuration and the computational results are accurate.

Acknowledgements

This work is part of the collaborative research project *Manufacturing of complex functional components with variants by using a new metal forming process - Sheet-Bulk Metal Forming* (SFB/TR73: www.tr-73.de).

References

[1] K. Bathe. *Finite Element Procedures: An Introduction to the Use of Finite Element Procedures*. Finite Element Procedures. Prentice Hall, 1996.

[2] M. Caspari, P. Landkammer, and P. Steinmann. Inverse from finding with h-adaptivity and an application to a notch stamping process. *Computational Plasticity XIV – Fundamentals and Applications (submitted)*, 2017.

[3] J.-L. Chenot, E. Massoni, and J. Fourment. Inverse problems in finite element simulation of metal forming processes. *Engineering Computations*, 13(2/3/4):190–225, 1996.

[4] E. Hinton and J. Campbell. Local and global smoothing of discontinuous finite element functions using a least squares method. *International Journal of Numerical Methods in Engineering*, 8(3):461–480, 1974.

[5] P. Landkammer, M. Caspari, and P. Steinmann. Improvements on a non-invasive, parameter-free approach to inverse form finding. *Computational Mechanics*, DOI: 10.1007/s00466-017-1468-2, 2017.

[6] P. Landkammer and P. Steinmann. A non-invasive heuristic approach to shape optimization in forming. *Computational Mechanics*, 57(2):169–191, 2016.

[7] M. Merklein, J. Allwood, B.-A. Behrens, A. Brosius, H. Hagenah, K. Kuzman, K. Mori, A. Tekkaya, and A. Weckenmann. Bulk forming of sheet metal. *CIRP Annals - Manufacturing Technology*, 61(2):725–745, 2012.

[8] P. Sieczkarek, S. Wernicke, S. Gies, P. A. F. Martins, and A. E. Tekkaya. Incipient and repeatable plastic flow in incremental sheet-bulk forming of gears. *The International Journal of Advanced Manufacturing Technology*, 9-12, 2016.

[9] U. Vierzigmann, J. Koch, M. Merklein, and U. Engel. Material flow in sheet-bulk metal forming. *Key Engineering Materials*, 504-506:1035–1040, 2012.

[10] Q. Yin, C. Soyarslan, A. Güner, A. Brosius, and A. E. Tekkaya. A cyclic twin bridge shear test for the identification of kinematic hardening parameters. *International Journal of Mechanical Sciences*, 59(1):31–43, 2012.